

Neutron star structure and collective excitations of finite nuclei

N. Paar^{1,*}, Ch. C. Moustakidis², T. Marketin¹, D. Vretenar¹, and G. A. Lalazissis²

¹*Physics Department, Faculty of Science, University of Zagreb, Croatia and*

²*Department of Theoretical Physics, Aristotle University of Thessaloniki, GR-54124 Thessaloniki, Greece*

(Dated: April 1, 2014)

We study relationships between properties of collective excitations in finite nuclei and the phase transition density n_t and pressure P_t at the inner edge separating the liquid core and the solid crust of a neutron star. A theoretical framework that includes the thermodynamic method, relativistic nuclear energy density functionals and the quasiparticle random-phase approximation is employed in a self-consistent calculation of (n_t, P_t) and collective excitations in nuclei. The covariance analysis shows that properties of charge-exchange dipole transitions, isovector giant dipole and quadrupole resonances and pygmy dipole transitions are correlated with the core-crust transition density and pressure. A set of relativistic nuclear energy density functionals, characterized by systematic variation of the density dependence of the symmetry energy of nuclear matter, is used to constrain possible values for (n_t, P_t) . By comparing the calculated excitation energies of giant resonances, energy weighted pygmy dipole strength, and dipole polarizability with available data, we obtain the weighted average values: $n_t = 0.0955 \pm 0.0007 \text{ fm}^{-3}$ and $P_t = 0.59 \pm 0.05 \text{ MeV fm}^{-3}$.

PACS numbers: 26.60.-c, 26.60.Gj, 24.30.Cz, 21.60.Jz, 21.65.Ef

The composition of the crust of a neutron star presents an interesting challenge both for nuclear structure physics as well as for nuclear astrophysics. A solid crust of $\approx 1 \text{ km}$ thickness and composed of nonuniform neutron-rich matter is located above a liquid core [1]. The crust presents an interface between observable surface phenomena and the invisible core of the star, and its structure can be related to interesting effects, such as glitches in the rotational period of pulsars, thermal relaxation after matter accretion, quasi periodic oscillations and anisotropic surface cooling [2]. The inner crust comprises the region from the density at which neutrons drip out from nuclei, to the inner edge separating the solid crust from the homogeneous liquid core. At the inner edge, in fact, a phase transition occurs from high-density homogeneous matter to inhomogeneous matter at lower densities. While the density at which neutrons drip out from nuclei is rather well determined, the transition density at the inner edge is much less certain because of insufficient knowledge of the equation of state of neutron-rich nuclear matter.

A number of theoretical studies have shown that the core-crust transition density and pressure are highly sensitive to the poorly constrained density dependence of the nuclear matter symmetry energy [3–6]. The symmetry energy that governs the composition of the neutron star crust, also determines the thickness of the neutron-skin $r_{np} = r_n - r_p$ in finite nuclei. In a model study of Ref. [3] an inverse correlation was found between the liquid-to-solid phase transition density for neutron-rich matter and the neutron-skin thickness of ^{208}Pb . Additional correlations between r_{np} and neutron star properties have also been investigated [7], including neutron star radii [8], the threshold density at the onset of the direct Urca process [9], and the crustal moment of inertia [7, 10]. Correlations between r_{np} and a variety of neutron star prop-

erties have recently been studied using covariance analysis based on relativistic energy density functional [11]. As pointed out by Horowitz and Piekarewicz [3], an accurate measurement of the neutron radius in ^{208}Pb by means of parity-violating electron scattering may have important implications for the structure of the crust of neutron stars. The parity radius experiment (PREX) has recently provided the first model-independent evidence for the neutron skin in ^{208}Pb [12]. However, since the experimental uncertainty of the PREX neutron skin thickness is very large ($r_{np} = 0.33^{+0.16}_{-0.18} \text{ fm}$), it will be useful to explore additional experimental constraints for neutron star properties. Here we focus on collective nuclear excitations that correlate with r_{np} and provide constraints on the symmetry energy.

The purpose of this Letter is to analyze possible relationships between collective excitation modes in finite nuclei and properties of the crust of a neutron star. Of particular importance are the liquid-to-solid transition density and pressure, that is, quantities that determine the inner region of the crust. Recent experimental studies of giant resonances, pygmy dipole resonances and other modes of excitation in nuclei, yielded a wealth of data that constrain the nuclear symmetry energy and neutron skin thickness [13]. Since there is a direct relation between the liquid-to-solid transition density and the neutron radius of ^{208}Pb [3], one expects that an analysis of the collective response of finite nuclei could also have important implications for the structure of the crust of neutron stars. This assumption will be put to the test in a theoretical framework that includes the thermodynamic method, relativistic nuclear energy density functionals and covariance analysis.

To determine the liquid-to-solid transition density for neutron-rich matter, the usual approach is to find the density at which the uniform liquid becomes unstable

against small-amplitude density fluctuations, indicating the formation of nuclear clusters. In this way a lower bound to the true transition density n_t is obtained [14]. The procedures used to determine n_t include the dynamic method [5, 14, 15], the thermodynamic method [4, 16–18], and the random-phase approximation (RPA) [3]. For the purpose of the present study the thermodynamic method will be employed. The constraint that determines the transition density is given by the inequality [4, 16]

$$C(n) = n^2 \frac{d^2 V}{dn^2} + 2n \frac{dV}{dn} + (1 - 2x)^2 \left[n^2 \frac{d^2 E_{sym}}{dn^2} + 2n \frac{dE_{sym}}{dn} - 2 \frac{1}{E_{sym}} \left(n \frac{dE_{sym}}{dn} \right)^2 \right] > 0, \quad (1)$$

where n , V , x and E_{sym} , denote the baryon density, the energy per particle of symmetric nuclear matter, the proton fraction, and the symmetry energy, respectively. The transition density n_t is determined by solving the equation $C(n_t) = 0$, and the corresponding transition pressure reads $P_t(n_t, x_t) = P_b(n_t, x_t) + P_e(n_t, x_t)$, where P_b , P_e are the baryon and electron contributions, respectively. x_t denotes the proton fraction that corresponds to n_t , and is computed using the condition of β -equilibrium [4]. For the analysis of correlations between the transition density and pressure (n_t , P_t) and observables that characterize collective excitations in finite nuclei, we consistently employ a relativistic nuclear energy density functional (RNEDF) to compute the energy per particle of symmetric nuclear matter and the symmetry energy, and in the RPA calculation of strength functions in finite nuclei. In this work the universal RNEDF with density-dependent meson-nucleon couplings [19] is used, and excitations in spherical nuclei are analyzed in the relativistic quasiparticle random phase approximation (RQRPA) [20]. The density dependence of the symmetry energy can be expressed in terms of coefficients of the Taylor expansion around nuclear matter saturation density n_0 :

$$E_{sym}(n) = E_{sym}(n_0) + L \left(\frac{n - n_0}{3n_0} \right) + \dots \quad (2)$$

where $E_{sym}(n_0) \equiv J$ is the symmetry energy at saturation, and L denotes the slope parameter. It has been shown that the parameters J, L correlate not only with the neutron-skin thickness of nuclei [21, 22], but also with neutron star properties [11, 23].

To assess the information content on the neutron star liquid-to-solid transition density and pressure, that is carried by various observables that characterize collective excitations in nuclei, the RNEDF and covariance analysis [24] are used to calculate correlations between quantities of interest. Covariance analysis is the least biased and most exhaustive approach to identify correlations between physical observables [11, 24]. For the

purpose of a covariance analysis the DDME-min1 parameterization of the RNEDF has been developed by fitting to ground-state data, that is, binding energies, charge radii, diffraction radii, and surface thickness of 17 spherical nuclei, from ^{16}O to ^{214}Pb [25]. Figure 1 shows the corresponding Pearson product-moment correlation coefficients [24] between the neutron star transition density n_t (and pressure P_t) and various quantities that characterize nuclear matter and finite nuclei. The correlation coefficients are obtained in a consistent implementation of the RNEDF and thermodynamic model, using the DDME-min1 parameterization. The following equilibrium nuclear matter properties are included: the binding energy at saturation density $E(n_0)$, the effective mass m/m^* , the incompressibility K , the symmetry energy J and slope of the symmetry energy at saturation L (Eq.(2)). Characteristic quantities of various modes of excitation of ^{208}Pb are also taken into consideration: the excitation energies of the isoscalar giant monopole resonance (ISGMR) and isoscalar giant quadrupole resonance (ISGQR), the dipole polarizability (α_D), the overall isovector dipole transition strength (m_0) and the respective energy-weighted dipole transition strength (m_1), the excitation energies of the isovector giant quadrupole resonance (IVGQR) and isovector giant dipole resonance (IVGDR), the m_1 moment (PDR m_1) and excitation energy (PDR - E) of the pygmy dipole strength function. In addition, the neutron-skin thickness (r_{np}) in ^{208}Pb is also included. The present covariance analysis confirms the strong linear correlation between n_t and the neutron-skin thickness of ^{208}Pb , as already shown in Ref. [3], and also displays a similar correlation between P_t and r_{np} . The results shown in Fig. 1 also indicate that collective excitations in finite nuclei are strongly correlated to the neutron star properties n_t and P_t . To constrain possible values of (n_t, P_t) , of particular interest are observables that simultaneously correlate with both quantities. These include the overall isovector dipole transition strength m_0 , the IVGDR and IVGQR excitation energies, the PDR energy weighted transition strength, and the dipole polarizability.

Figure 1 shows that the liquid-to-solid transition density and pressure are also correlated with the symmetry energy coefficients J and L . It is, therefore, interesting to analyze how various excitation modes in nuclei, that limit possible values of r_{np} , provide constraints on the density dependence of the symmetry energy. Similar studies have recently been performed for different modes of excitation using the framework of energy density functionals (e.g. Refs. [26–28]). In the present analysis a consistent set of RNEDFs that span a range of values $J = 30 - 38$ MeV and $L = 30 - 110.8$ MeV [29], is employed in a calculation of collective excitations. The set of RNEDFs was adjusted to accurately reproduce nuclear-matter properties, binding energies and charge radii of a standard set of spherical nuclei, but with constrained

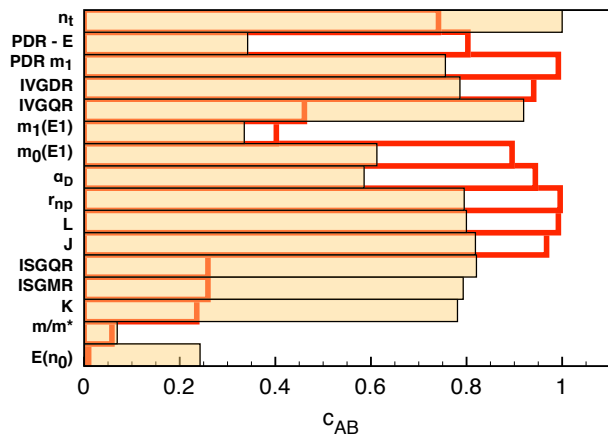


FIG. 1: (Color online). Pearson product-moment correlation coefficients between the density n_t (shaded bars - thin lines) at the phase transition between the liquid core and the solid crust of a neutron star, and various observables of collective excitations for ^{208}Pb and nuclear matter properties. The corresponding correlation coefficients for the pressure P_t are displayed by thick (red) bars.

values for the symmetry energy J and slope parameter L [29]. These functionals were recently used to constrain the density dependence of the nuclear symmetry energy and the neutron-skin thickness from the observed pygmy dipole strength ($^{130,132}\text{Sn}$) [30], and the anti-analog giant dipole resonance (^{208}Pb) [31]. By performing self-consistent relativistic mean-field calculations for the nuclear ground states, and the corresponding RQRPA for collective excitations, we have computed the AGDR and IVGQR excitation energies in ^{208}Pb , the dipole polarizability α_D of ^{208}Pb , and the PDR transition strength in ^{68}Ni . For the set of RNEDFs, linear correlations are established between the calculated characteristics of collective excitations and the symmetry energy J and slope parameter L , in agreement with the results of the covariance analysis shown in Fig. 1. These correlations, together with the corresponding experimental results on the excitation strengths and energies [31–34], provide independent constraints on J and L , shown in Fig. 2. For comparison we also include the results of a previous study that was based on the same set of RNEDFs, but used data on the PDR in $^{130,132}\text{Sn}$ [30]. Figure 2 shows that all calculated excitation properties consistently constrain possible values of J and L , with differences attributed to variations of the experimental uncertainties. It is interesting to note that all results overlap in a narrow region of the (J, L) plane. The weighted average yields $J = 32.5 \pm 0.5$ MeV and $L = 49.9 \pm 4.7$ MeV. More accurate experimental results would, of course, further reduce the uncertainties shown in Fig. 2.

In the next step we use the same set of RNEDFs to compute the liquid-to-solid transition density and pressure in the thermodynamic approach of Eq. (1). In Fig. 3

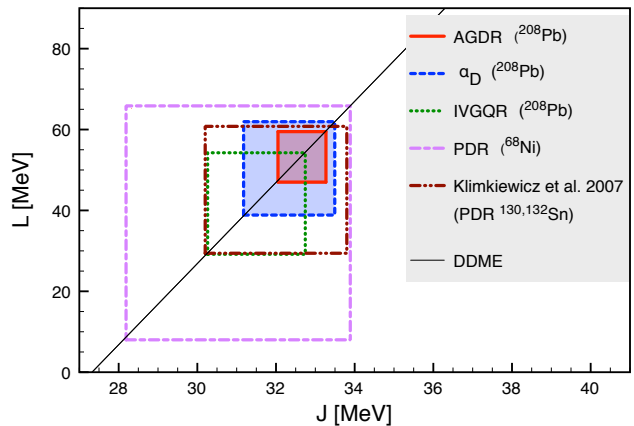


FIG. 2: (Color online). Constraints of the symmetry energy at saturation J and the slope parameter L , obtained from a comparison of RNEDF results and data on AGDR [35] and IVGQR [32] excitation energies (^{208}Pb), the dipole polarizability α_D of ^{208}Pb [33], and the PDR energy weighted strength (^{68}Ni [34], $^{130,132}\text{Sn}$ [30]).

the transition pressure P_t is plotted as a function of the transition density n_t , and we notice the particular linear dependence predicted by the DDME set of relativistic functionals. The rectangles denote the values of P_t and n_t , that is, the corresponding energy density functionals, that in a consistent RQRPA calculation reproduce data on collective excitations within experimental uncertainties: the AGDR [31] and IVGQR [32] excitation energies (^{208}Pb), the dipole polarizability α_D (^{208}Pb) [33], and the PDR energy weighted strength (^{68}Ni) [34]. One notices that collective excitations provide rather stringent constraints on the possible values of P_t and n_t , and there is even a small region in the (P_t, n_t) plane in which all constraints overlap. Obviously, more accurate measurements of charge-exchange modes and pygmy dipole strength are necessary to reduce current uncertainties but, nevertheless, the weighted average from the present analysis yields $n_t = 0.0955 \pm 0.0007 \text{ fm}^{-3}$ and $P_t = 0.59 \pm 0.05 \text{ MeV fm}^{-3}$.

For comparison, Fig. 3 also includes constraints on (P_t, n_t) obtained by other methods, based on modified Gogny (MDI) interactions [5, 35], Dirac-Brueckner-Hartree-Fock (DBHF) calculations [36], and RNEDF calculations supplemented with constraints from the empirical range for the slope parameter L and neutron-skin thickness in Sn isotopes and ^{208}Pb [4]. We note that a previous study based on the $A18 + \delta v + \text{UIX}^*$ interaction predicted a somewhat lower value for the transition density: $n_t = 0.087 \text{ fm}^{-3}$ [37], whereas the constraints obtained in the present analysis are consistent with the result based on the nonrelativistic microscopic equation of state of Friedman and Pandharipande [38]: $n_t = 0.096 \text{ fm}^{-3}$ [39].

In conclusion, using a theoretical framework based on

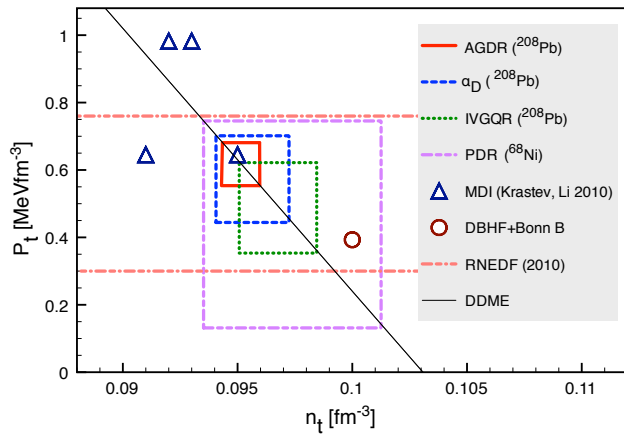


FIG. 3: (Color online). The liquid-to-solid transition pressure P_t for neutron-rich matter as a function of the transition density n_t . The rectangles correspond to the values of (P_t, n_t) calculated using the RNEDF and experimental data for AGDR [31] and IVGQR [32] excitation energies (^{208}Pb), the dipole polarizability α_D (^{208}Pb) [33], and the PDR energy weighted strength (^{68}Ni) [34]. Results obtained by several other methods: the MDI interactions [5, 35], DBHF+Bonn B calculations [36], and the self-consistent RNEDF calculation [4], are shown for comparison.

nuclear density functional theory, it is shown that the neutron star liquid-to-solid phase transition density and pressure are correlated with properties of collective excitations in finite nuclei. A set of RNEDFs characterized by systematic variation of the density dependence of the symmetry energy, is used in a self-consistent RPA calculation of charge-exchange transitions, isovector giant quadrupole resonances, pygmy dipole transitions and dipole polarizability. A comparison with available data yields the following weighted average values for the symmetry energy at saturation $J = 32.5 \pm 0.5$ MeV, and the slope parameter $L = 49.9 \pm 4.7$ MeV. Using the thermodynamic method, the same set of RNEDFs predicts a particular linear dependence of the phase transition density n_t and pressure P_t at the inner edge between the liquid core and the solid crust of a neutron star. By comparing the corresponding RPA theoretical values for the AGDR and IVGQR excitation energies (^{208}Pb), the dipole polarizability α_D (^{208}Pb), and the PDR energy weighted strength (^{68}Ni) with available data, one obtains rather stringent constraints on the possible values: $n_t = 0.0955 \pm 0.0007 \text{ fm}^{-3}$ and $P_t = 0.59 \pm 0.05 \text{ MeV fm}^{-3}$. Of course, the present analysis has been based on a single family of RNEDFs with the aim to demonstrate the feasibility of the proposed theoretical approach. Further extensive studies with a wider range of non-relativistic and relativistic functionals will provide more robust quantitative estimates of the liquid-to-solid transition density and pressure. This method crucially depends on experimental uncertainties of ob-

servables that characterize collective modes of excitation and, therefore, accurate measurements are necessary to further constrain the structure of the neutron star crust.

* Electronic address: npaar@phy.hr

- [1] P. Haensel, A.Y. Potekhin, and D.G. Yakovlev, *Neutron Stars 1: Equation of State and Structure* (Springer-Verlag, New York, 2007).
- [2] J.M. Lattimer and M. Prakash, *Phys. Rep.* **333**, 121 (2000).
- [3] C. J. Horowitz, J. Piekarewicz, *Phys. Rev. Lett.* **86**, 5647 (2001).
- [4] Ch. C. Moustakidis, T. Nikšić, G. A. Lalazissis, D. Vretenar, and P. Ring, *Phys. Rev. C* **81**, 065803 (2010).
- [5] J. Xu, L. W. Chen, B. A. Li, and H. R. Ma, *Astrophys. J.* **697**, 1549 (2009).
- [6] C. Ducoin, J. Margueron, C. Providencia, I. Vidana, *Phys. Rev. C* **83**, 045810 (2011).
- [7] A. W. Steiner, M. Prakash, J. M. Lattimer, and P. J. Ellis, *Phys. Rep.* **411**, 325 (2005).
- [8] J. Carriere, C. J. Horowitz, and J. Piekarewicz, *Astrophys. J.* **593**, 463 (2003).
- [9] C. J. Horowitz and J. Piekarewicz, *Phys. Rev. C* **66**, 055803 (2002).
- [10] F. J. Fattoyev and J. Piekarewicz, *Phys. Rev. C* **82**, 025810 (2010).
- [11] F. J. Fattoyev and J. Piekarewicz, *Phys. Rev. C* **86**, 015802 (2012).
- [12] S. Abrahamyan et al., *Phys. Rev. Lett.* **108**, 112502 (2012).
- [13] D. Savran, T. Aumann, A. Zilges, *Prog. Part. Nucl. Phys.* **70**, 210 (2013).
- [14] C. J. Pethick, D. G. Ravenhall, and C. P. Lorenz, *Nucl. Phys. A* **584**, 675 (1995); F. Douchin and P. Haensel, *Phys. Lett. B* **485**, 107 (2000).
- [15] C. Ducoin, Ph. Chomaz, and F. Gulminelli, *Nucl. Phys. A* **789**, 403 (2007).
- [16] J. M. Lattimer and M. Prakash, *Phys. Rep.* **442**, 109 (2007).
- [17] S. Kubis, *Phys. Rev. C* **76**, 025801 (2007).
- [18] A. Worley, P.G. Krastev, and B.A. Li, *Astrophys. J.* **685**, 390 (2008).
- [19] T. Nikšić, D. Vretenar, P. Finelli, and P. Ring, *Phys. Rev. C* **66**, 024306 (2002).
- [20] N. Paar, D. Vretenar, E. Khan, and G. Colò, *Rep. Prog. Phys.* **70**, 691 (2007).
- [21] R. J. Furnstahl, *Nucl. Phys. A* **706**, 85 (2002).
- [22] M. Centelles, X. Roca-Maza, X. Vinas, and M. Warda, *Phys. Rev. Lett.* **102**, 122502 (2009).
- [23] F. J. Fattoyev and J. Piekarewicz, *Phys. Rev. C* **84**, 064302 (2011).
- [24] P.-G. Reinhard and W. Nazarewicz, *Phys. Rev. C* **81**, 051303(R) (2010).
- [25] X. Roca-Maza, N. Paar, G. Colò, to appear in *J. Phys. G* (2014).
- [26] A. Carbone, G. Colò, A. Bracco et al., *Phys. Rev. C* **81**, 041301(R) (2010).
- [27] M. B. Tsang et al., *Phys. Rev. C* **86**, 015803 (2012).
- [28] X. Roca-Maza, M. Brenna, B. K. Agrawal et al., *Phys. Rev. C* **87**, 034301 (2013).

- [29] D. Vretenar, T. Nikšić, P. Ring, Phys. Rev. C **68**, 024310 (2003).
- [30] A. Klimkiewicz et al., Phys. Rev. C **76**, 051603(R) (2007).
- [31] A. Krasznahorkay et al., arXiv:1311.1456 (2014).
- [32] S. S. Henshaw et al., Phys. Rev. Lett. **107**, 222501 (2011).
- [33] A. Tamii et al., Phys. Rev. Lett. **107**, 062502 (2011).
- [34] O. Wieland, A. Bracco, F. Camera et al., Phys. Rev. Lett. **102**, 092502 (2009).
- [35] P. G. Krastev and B. A. Li, arXiv:1001.0353 [astro-ph.SR].
- [36] F. Sammarruca and P. Liu, Phys. Rev. C **79**, 057301 (2009); F. Sammarruca, arXiv:1002.0146 [nucl-th].
- [37] A. Akmal, V. R. Pandharipande, and D. G. Ravenhall, Phys. Rev. C **58**, 1804 (1998).
- [38] B. Friedman and V. R. Pandharipande, Nucl. Phys. A **631**, 502 (1981).
- [39] C. P. Lorenz, D. G. Ravenhall, and C. J. Pethick, Phys. Rev. Lett. **70**, 379 (1993).